



**HAL**  
open science

# Discretized Keiper/Li approach to the Riemann Hypothesis

André Voros

► **To cite this version:**

André Voros. Discretized Keiper/Li approach to the Riemann Hypothesis. *Experimental Mathematics*, 2018, 10.1080/10586458.2018.1482480 . cea-01696126

**HAL Id: cea-01696126**

**<https://cea.hal.science/cea-01696126>**

Submitted on 30 Jan 2018

**HAL** is a multi-disciplinary open access archive for the deposit and dissemination of scientific research documents, whether they are published or not. The documents may come from teaching and research institutions in France or abroad, or from public or private research centers.

L'archive ouverte pluridisciplinaire **HAL**, est destinée au dépôt et à la diffusion de documents scientifiques de niveau recherche, publiés ou non, émanant des établissements d'enseignement et de recherche français ou étrangers, des laboratoires publics ou privés.

# Discretized Keiper/Li approach to the Riemann Hypothesis

**André Voros**

Institut de physique théorique, Université Paris-Saclay, CEA, CNRS  
F-91191 Gif-sur-Yvette Cedex (France)

E-mail: `andre.voros@ipht.fr`

July 18, 2017

## Abstract

The Keiper–Li sequence  $\{\lambda_n\}$  is most sensitive to the Riemann Hypothesis asymptotically ( $n \rightarrow \infty$ ), but highly elusive both analytically and numerically. We deform it to fully explicit sequences, simpler to analyze and to compute (up to  $n = 5 \cdot 10^5$  by G. Misguich). We extend that to the Davenport–Heilbronn counterexamples, then demonstrate explicit tests that selectively react to zeros *off* the critical line.

The present text develops our computations announced from 2015 [34].

## 1 Main notations and background

- $\zeta(x)$  : the Riemann zeta function,  $x \in \mathbb{C} \setminus \{1\}$ ; (e.g., [30][10, chap. 8, 15])
- $2\xi(x)$  : a completed zeta function, obeying Riemann’s Functional Equation,

$$2\xi(x) \stackrel{\text{def}}{=} x(x-1)\pi^{-x/2}\Gamma(x/2)\zeta(x) \equiv 2\xi(1-x), \quad (1)$$

and better normalized for us than Riemann’s  $\xi$ -function:  $2\xi(0) = 2\xi(1) = 1$ . The symmetry in (1) makes us also denote  $x = \frac{1}{2} + t + iT$  ( $t, T$  real).

- $\{\rho\}$  : the set of zeros of  $\xi$  (the *nontrivial zeros* of  $\zeta$  or *Riemann zeros*, counted with multiplicities if any); this set has the symmetry axes  $\mathbb{R}$  and

$L \stackrel{\text{def}}{=} \{\text{Re } x = \frac{1}{2}\}$  (the *critical line*), it lies in the *critical strip*  $\{0 < \text{Re } x < 1\}$ , and its ordinate-counting function  $N(T) \stackrel{\text{def}}{=} \#\{\rho \mid 0 \leq \text{Im } \rho \leq T\}$  has the *Riemann-von Mangoldt* asymptotic form

$$N(T) = \frac{T}{2\pi} \left( \log \frac{T}{2\pi} - 1 \right) + O(\log T), \quad T \rightarrow +\infty; \quad (2)$$

infinite summations over zeros are to be ordered symmetrically, as

$$\sum_{\rho} \stackrel{\text{def}}{=} \lim_{T \rightarrow \infty} \sum_{|\text{Im } \rho| \leq T} . \quad (3)$$

• **The Riemann Hypothesis (RH):** *for all* Riemann zeros,  $\text{Re } \rho \equiv \frac{1}{2}$ . [26] This remains a major open problem. Up to *bounded* heights  $|\text{Im } \rho| < T_0$  on the other hand,  $\text{Re } \rho \equiv \frac{1}{2}$  has been systematically confirmed (by direct checking), with  $T_0$  having currently reached the value [15]

$$T_0 \approx 2.4 \cdot 10^{12} \quad (\text{as of 2004}). \quad (4)$$

Our goal is to present a novel type of *explicit* sequential criteria for RH, and to see how these might work to test RH *further* (i.e., beyond  $T_0$ ).

We will dub  $\rho'$  any zeros for which we assume  $\text{Re } \rho' > \frac{1}{2}$  (violating RH).

•  $k!!$  : the double factorial, used here for odd integers  $k$  only, in which case

$$\begin{aligned} k!! &\stackrel{\text{def}}{=} k(k-2) \cdots 1 && \text{for odd } k > 0, \\ &\stackrel{\text{def}}{=} 2^{(k+1)/2} \Gamma(\frac{1}{2}k + 1) / \sqrt{\pi} && \text{for odd } k \geq 0 \quad (\text{e.g., } (-1)!! = 1). \end{aligned} \quad (5)$$

•  $B_{2m}$  : Bernoulli numbers ( $m = 0, 1, 2, \dots$ );  $\gamma$  : Euler's constant.

## 1.1 The Keiper and Li coefficients

In 1992 Keiper [18] considered a real sequence  $\{\lambda_n\}$  of generating function

$$\varphi(z) \stackrel{\text{def}}{=} \log 2\xi(M(z)) \equiv \sum_{n=1}^{\infty} \lambda_n^K z^n, \quad M(z) \stackrel{\text{def}}{=} \frac{1}{1-z}, \quad (6)$$

(we write  $\lambda_n^K$  for *Keiper's*  $\lambda_n$ ), deduced that

$$\lambda_n^K \equiv n^{-1} \sum_{\rho} [1 - (1 - 1/\rho)^n], \quad (7)$$

and that  $\text{RH} \Rightarrow \lambda_n^K > 0$  ( $\forall n$ ), then asserted (without proof nor elaboration): “if we assume the Riemann hypothesis, and further that the zeros are very evenly distributed, we can show that  $\lambda_m \approx \frac{\log m}{2} - \frac{\log(2\pi) + 1 - \gamma}{2}$ .” I.e.,

$$\lambda_m^K \approx \frac{1}{2} \log m + c, \quad c = \frac{1}{2}(\gamma - \log 2\pi - 1) \approx -1.130330700754. \quad (8)$$

The conformal mapping  $M : z \mapsto x$  in (6) pulls back each zero  $\rho$  to

$$z_\rho \stackrel{\text{def}}{=} M^{-1}(\rho) = 1 - 1/\rho, \quad (9)$$

and *the critical line  $L$  to the unit circle  $\{|z| = 1\}$* , ensuring that (Fig. 1):

$$\text{RH} \iff |z_\rho| \equiv 1 \ (\forall \rho) \iff \varphi \text{ is regular in the full disk } \{|z| < 1\}. \quad (10)$$

In 1997 Li [20] independently introduced another sequence  $\{\lambda_n\}$ , through

$$\lambda_n^L = \frac{1}{(n-1)!} \frac{d^n}{dx^n} [x^{n-1} \log 2\xi(x)]_{x=1}, \quad n = 1, 2, \dots, \quad (11)$$

(we write  $\lambda_n^L$  for *Li's*  $\lambda_n$ ), deduced that

$$\lambda_n^L \equiv \sum_{\rho} [1 - (1 - 1/\rho)^n], \quad (12)$$

and proved the *sharp equivalence (Li's criterion)*:

$$\text{RH} \iff \lambda_n^L > 0 \text{ for all } n. \quad (13)$$

As seen for instance by comparing (7) vs (12),

$$\lambda_n^L \equiv n \lambda_n^K \quad \text{for all } n = 1, 2, \dots; \quad (14)$$

our superscripts K vs L will disambiguate  $\lambda_n$  whenever the factor  $n$  matters.

## 1.2 Probing RH through the Keiper–Li constants $\lambda_n$

Li's criterion (13) makes it clear that the Keiper–Li sequence is *RH-sensitive*: does it then provide new and more efficient ways to test RH?

Known results actually entail that, beyond the present frontier (4), the sequence  $\{\lambda_n\}$  may effectively probe RH only in its *tail*  $n \gg 1$  and via its *asymptotic form* for  $n \rightarrow \infty$ .

In 2000 Oesterlé proved (but left unpublished) that [25, prop. 2][5, § 2.3]

$$\operatorname{Re} \rho = \frac{1}{2} \text{ for all zeros with } |\operatorname{Im} \rho| \leq T_0 \implies \lambda_n \geq 0 \text{ for all } n \leq T_0^2, \quad (15)$$

and that under RH, [25, § 2]

$$\lambda_n^L = n\left(\frac{1}{2} \log n + c\right) + o(n)_{n \rightarrow \infty} \quad \text{with } c = \frac{1}{2}(\gamma - \log 2\pi - 1), \quad (16)$$

which concurs with Keiper's formula (8) but now assuming *RH alone*.

In 2004 Maślanka [21][22] computed a few thousand  $\lambda_n^L$ -values numerically and inferred asymptotic conjectures on them for the case RH true.

In 2004–2006, inspired by the latter (but unaware of [25]), we used the saddle-point method to draw an *asymptotic criterion* for RH: [31] as  $n \rightarrow \infty$ ,

- RH false:  $\lambda_n^L \sim - \sum_{\operatorname{Re} \rho' > \frac{1}{2}} z_{\rho'}^{-n} \pmod{o(r^{-n}) \forall r < 1}$  (17)

(exponentially growing oscillations *with both signs*);<sup>1</sup>

- RH true:  $\lambda_n^L \sim n\left(\frac{1}{2} \log n + c\right) \pmod{o(n)}$  (18)  
(implying asymptotic *positivity*).

Note: the remainder term  $o(n)$  in (16) got improved to  $O(\sqrt{n} \log n)$  by Lagarias [19] (2007), and to  $ny_n$  with  $\{y_n\} \in \ell^2$  by Arias de Reyna [1] (2011).

Hence, even with the (fixed) sequence  $\{\lambda_n\}$ , violations of RH will get increasingly harder to track as the floor height  $T_0$  (currently (4)) gets higher.

First, Li's sign test (13) is, by (15), inactive up to  $n = T_0^2$  ( $\approx 5 \cdot 10^{24}$  today) at least. As for the asymptotic alternative (17)–(18): if a zero  $\rho' = \frac{1}{2} + t + iT$  violates RH then  $|T| \geq T_0 \gg 1$ , and the effect  $z_{\rho'}^{-n}$  in (17) becomes detectable against the background (18) only for  $n \gtrsim T^2/|t|$ . [32] Now in the  $z$  variable, that RH-violation is measured by  $\delta|z| = |z_{\rho'}| - 1$  (Fig. 1 right); but  $\delta|z|/|z| \approx |t|/T^2$  as  $|T| \gg 1$ , therefore  $n \gtrsim T^2/|t|$  means  $n|\delta \log |z|| \gtrsim 1$

---

<sup>1</sup>Erratum: in [31][32] we missed the overall  $(-)$  sign (with no effect on our conclusions), which we rectified in [33].

which is no less than the *uncertainty principle*, as  $(i \log z)$  and  $n$  are Fourier-conjugate variables in (6). Then, as that principle is universal,  $n \gtrsim T^2/|t|$  will bound *any* detection of  $\rho'$  through  $\lambda_n$ . With  $|t| < \frac{1}{2}$ , the best possible sensitivity domain of  $\{\lambda_n\}$  to RH is, finally,

$$n \gtrsim 2T_0^2, \quad \text{currently implying } n \gtrsim 10^{25}. \quad (19)$$

It is then no surprise that published  $\lambda_n$ -plots (having  $n \lesssim 7000$ ) solely reflect the RH-true pattern (18) (already from  $n \approx 30$ ). [18][21]

So, whether one would take (13) or (17)–(18) to track violations of RH, the Keiper–Li sequence  $\{\lambda_n\}$  only matters in its *asymptotic tail*  $\{n \gg 1\}$ , where the alternative (17)–(18) rules (and enacts Li’s sign property as well).

At the same time, the  $\lambda_n$  are quite elusive analytically [7][9]. Numerically too, (see Maślanka [21][22] and Coffey [8]) their evaluation requires a recursive machinery, of intricacy blowing up with  $n$ ; [22, fig. 6] moreover reports a loss of ca. 0.2 decimal place of precision per step  $n$  (when working *ex nihilo* - i.e., using no Riemann zeros in input); only  $\lambda_n$ -values up to  $n \approx 4000$  were thus accessed until recently, with  $n = 10^5$  attained by Johansson [17, § 4.2] (who states a loss of 1 bit  $\approx 0.3$  decimal place per step  $n$ ). Even then, the range (19) needed for new tests of RH stays out of reach, motivating quests for more accessible sequences.

But first, as the *asymptotic* sensitivity to RH is the main property we will prove to generalize, we review its mechanism for  $\{\lambda_n\}$  itself.

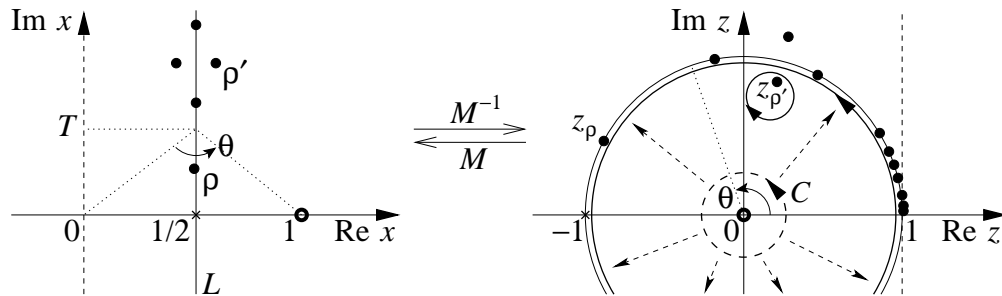


Figure 1: Riemann zeros ( $\bullet$ ) depicted *schematically* in the  $x$  (left) and  $z$  (right) upper half-planes (at mock locations, including a putative pair off the critical line  $L$ ). Symmetrical lower half-planes, and the zeros therein, are implied. In the  $z$ -plane (right), we also plot the contour deformation used by Darboux’s method upon the integral (21) for  $n \rightarrow \infty$ .

### 1.3 Asymptotic analysis of $\{\lambda_n\}$ (to be generalized)

The forthcoming derivation of the large- $n$  alternative (17)–(18) for  $\lambda_n$  readily settles the RH-false case (17), then needs one more step for the RH-true formula (18). (In [31] we obtained both cases in parallel by the saddle-point method used on a single integral, but this approach does not yet extend.)

Within the broader setting of large-order asymptotics, we basically follow the classic Darboux’s idea [12, § 7.2]: for a sequence like (6), the  $n \rightarrow \infty$  form is ruled by the radius of convergence of its generating function  $\varphi(z)$ , by use of the integral formula (equivalent to (6) by the residue theorem)

$$\lambda_n^K = \frac{1}{2\pi i} \oint_C \frac{dz}{z^{n+1}} \varphi(z), \quad \varphi(z) \equiv \log 2\xi\left(\frac{1}{1-z}\right), \quad (20)$$

where  $C$  is a positive contour close to  $z = 0$  leaving all other singularities (namely, those of  $\varphi(z)$ ) outside.

#### 1.3.1 Darboux’s method does the RH false case

Solely for this stage, it is worth integrating (20) by parts first, to

$$\lambda_n^L = (2\pi i)^{-1} \oint_C z^{-n} \varphi'(z) dz : \quad (21)$$

$\varphi'$ , a meromorphic function, will be simpler to use than the multiply-valued  $\varphi$ .

Since the integrand in (21) has the large- $n$  form  $e^{\Phi_n(z)}$  where  $\Phi_n$  tends to  $\infty$  with  $n$  ( $\Phi_n(z) \sim -n \log z$ ), we may use the steepest-descent method [13, § 2.5] to deform the contour  $C$  toward decreasing  $\text{Re}(-n \log z)$ , i.e., as a circle of radius  $r$  growing toward 1 (Fig. 1 right); then, by the residue theorem, each singularity of  $\varphi'$  swept in turn, namely a simple pole  $z_{\rho'}$  per RH-violating zero  $\rho'$  on the  $\{\text{Re } x > \frac{1}{2}\}$  side, yields an asymptotic contribution ( $-z_{\rho'}^{-n}$ ) in descending order, and these altogether add up to (17). [31]

If now RH is true, then as the radius of the contour attains  $r = 1^-$ , (17) reaches no better than  $\lambda_n^L = o(r^{-n})$  ( $\forall r < 1$ ); only a finer analysis of the limiting integral at  $r = 1^-$  pins down an asymptotic form for  $\lambda_n$ , see next.

#### 1.3.2 Oesterlé’s argument for the RH true case [25]

(reworded by us). Its starting point will be the real-integral form (22) below, which comes from letting the contour in (20) go up to  $\{|z| = 1^-\}$

(unobstructed, under RH true), making the change of variable  $z = e^{i\theta}$ , and reducing to an integral over real  $\theta$ : [25][31]

$$\lambda_n^K = 2 \int_0^\pi \sin n\theta N\left(\frac{1}{2} \cot\left(\frac{1}{2}\theta\right)\right) d\theta. \quad (22)$$

Now,  $\theta$  real  $\iff M(z) = \frac{1}{2} + iT$  with real  $T \equiv \frac{1}{2} \cot \frac{1}{2}\theta$ , so  $\theta$  is also the angle subtended by the real vector  $(\overrightarrow{01})$  from the point  $\frac{1}{2} + iT$  (Fig. 1 left); the counting function condenses to the critical line:  $N(T) \equiv \#\{\rho \in [\frac{1}{2}, \frac{1}{2} + iT]\}$ . An alternative validation of (22) is that its (Stieltjes) integral by parts  $n^{-1} \int_0^\pi 2(1 - \cos n\theta) dN$  at once yields the sum formula (7) under RH.

The  $n \rightarrow \infty$  form mod  $o(1)$  of (22) now directly stems from the Riemann–von Mangoldt formula (2),  $N(T) = \frac{T}{2\pi} (\log \frac{T}{2\pi} - 1) + O(\log T)_{T \rightarrow +\infty}$ :

1)  $O(\log T)$  is integrable in  $\theta$  up to  $\theta = 0$ , hence the Riemann–Lebesgue lemma says that its integral against  $\sin n\theta$  in (22) is  $o(1)$ , i.e., negligible;

2) we change to the variable  $\Theta_n \equiv n\theta$ ; then, change the resulting upper integration bound  $n\pi$  to  $+\infty$  and use  $T \sim 1/\theta = n/\Theta_n$ , all mod  $o(1)$ , to get

$$\lambda_n^K \sim \int_0^\infty 2 \sin \Theta_n \frac{n}{2\pi\Theta_n} \left[ \log \frac{n}{2\pi\Theta_n} - 1 \right] \frac{d\Theta_n}{n} \pmod{o(1)}. \quad (23)$$

This finally reduces, by the classic formulae  $\int_0^\infty \sin \Theta d\Theta/\Theta = \pi/2$  and  $\int_0^\infty \sin \Theta \log \Theta d\Theta/\Theta = -\pi\gamma/2$  [16, eqs. (3.721(1)) and (4.421(1))], to

$$\lambda_n^K = \frac{1}{2} \log n + c + o(1) \quad (\text{under RH true}), \quad (24)$$

amounting to (16). □

## 2 An *explicit* variant to the sequence $\{\lambda_n^K\}$

Given those difficulties with the original sequence  $\{\lambda_n\}$  (§ 1.2), we propose to *deform* it (specifically, *Keiper's* form (6)) into a simpler one, still RH-sensitive but of *elementary closed form*.

While the original specification (6) for  $\lambda_n$  looks *rigid*, this is due to an extraneous assumption implied on the mapping  $M$ : that the  $x$ -plane image  $x_0 \stackrel{\text{def}}{=} M(z=0)$  has to be the pole of  $\zeta$ , i.e.,  $x_0 \equiv 1$ . Indeed, (6) at once builds  $\{\lambda_n\}$  upon the germ of  $\log 2\xi(x)$  at  $x_0 = M(0)$  (“basepoint” for  $\{\lambda_n\}$ ), and fixes  $M(0) \equiv 1$  but *this* imposition is only optional. To wit, (6) with

other conformal mappings  $\widetilde{M} \neq M$  gives RH-sensitivity just as well: the key condition is (10), fulfilled if  $\widetilde{M}^{-1}(\{\rho\} \cap L) \subset \{|z| = 1\}$ , and this nowhere binds the basepoint  $x_0$  (now:  $\widetilde{M}(0)$ ). Prime such examples are all  $\widetilde{M} = M \circ H_{\tilde{z}}$ , where  $H_{\tilde{z}}$  conformally maps the unit disk onto itself as

$$z \mapsto H_{\tilde{z}}(z) \stackrel{\text{def}}{=} (z - \tilde{z}) / (1 - \tilde{z}^* z) \quad (\text{Möbius transformation}); \quad (25)$$

these  $\widetilde{M}$ , for which  $x_0 = (1 + \tilde{z})^{-1}$ , yield *parametric* coefficients  $\lambda_n(x_0)$  in terms of the derivatives  $(\log \xi)^{(m)}(x_0)$ ; those are in fact Sekatskii's [27] "generalized Li's sums"  $k_{n,a}$  with  $x_0 \equiv (1 - a) \in \mathbb{R} \setminus \{\frac{1}{2}\}$ . Independently, different (double-valued) conformal mappings  $\widetilde{M}$  yield "centered"  $\lambda_n^0$  of basepoint precisely  $x_0 = \frac{1}{2}$ , the symmetry center for  $\xi(x)$  ([33, § 3.4], and Appendix).

But to attain truly simpler and explicit results, neither of those alterations goes far enough. As a further step, rather than depending on a single basepoint (except, in a loose sense,  $x_0 = \infty$ ?), we will crucially *discretize* the derivatives of  $\log \xi$  within the original  $\lambda_n$  into selected *finite differences* (and likewise in the Appendix for our centered  $\lambda_n^0$ ).

## 2.1 Construction of a new sequence $\{\Lambda_n\}$

The  $\lambda_n$  are quite elusive as they involve *derivatives* of  $\log 2\xi$  (and worse, of growing order), cf. (11). On the integral form (20), that clearly ties to the denominator  $z^{n+1}$  having its zeros *degenerate* (all at  $z = 0$ , see fig. 2 left).

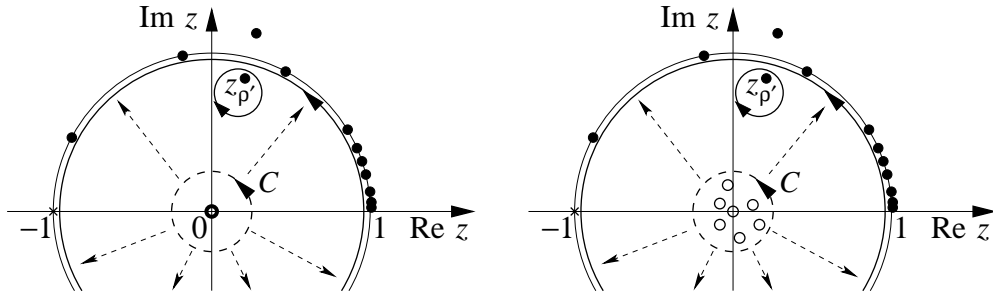


Figure 2: As Fig. 1 right, but now showing the multiple pole  $z = 0$  (left plot) split into simple ones (right plot) without disrupting the large- $n$  analysis of § 1.3.

Now at given  $n$ , if we *split those zeros apart* as  $0, z_1, \dots, z_n$  (all distinct, and still inside the contour: fig. 2 right), then by the residue theorem, (20) will simplify to a linear combination of the  $\varphi(z_m)$ , i.e., a *finite difference*.

Doing so by plain shifts of the factors  $z \mapsto z - z_m$  would also split their unit disks apart, and thus ruin the setting of § 1.3 for asymptotic RH-sensitivity. So to fix  $\{|z| = 1\}$ , we again use *hyperbolic* translations (25), but now *a different one upon each factor*:  $z \mapsto H_{z_m}(z)$ , instead of a common one on all of  $z^{n+1}$  as done formerly (which left  $\log 2\xi$  differentiated, only elsewhere).

The origin  $z = 0$  has then lost all special status, hence so does the particular mapping  $M$  (selected to make  $z = 0$  the preimage of the pole  $x = 1$ ); then the variable  $x$ , natural for the  $\zeta$ -function, is also the simplest to use here. Rewritten in the variable  $x$ , (20) reads as

$$\lambda_n^K = \frac{1}{2\pi i} \oint \frac{dx}{x(x-1)} \left(\frac{x}{x-1}\right)^n \log 2\xi(x) \quad (\text{integrated around } x = 1), \quad (26)$$

and the deformations just introduced have the form

$$\frac{1}{2\pi i} \oint_{\mathcal{C}_n} \frac{dx}{x(x-1)} \frac{1}{h_{x_1}(x) \dots h_{x_n}(x)} \log 2\xi(x), \quad h_{\tilde{x}}(x) \equiv \frac{\tilde{x}^*}{\tilde{x}} \frac{x - \tilde{x}}{x + \tilde{x}^* - 1}, \quad (27)$$

where the contour  $\mathcal{C}_n$  encircles the set  $\{1, x_1, \dots, x_n\}$  positively (and may as well depend on  $n$ ). Then the integral in (27) readily evaluates to

$$\sum_{m=1}^n \operatorname{Res}_{x=x_m} f_n(x) \log 2\xi(x_m), \quad f_n(x) \stackrel{\text{def}}{=} \frac{1}{x(x-1)} \frac{1}{[h_{x_1} \dots h_{x_n}](x)}, \quad (28)$$

by the residue theorem ( $x = 1$  contributes zero thanks to  $\log 2\xi(1) = 0$ ).

Now, we choose  $x_m \equiv 2m$  for  $m = 1, 2, \dots$  (independently of  $n$ ), to capitalize on the known values  $\zeta(2m)$ . That fixes

$$f_n(x) = \frac{g_n(x)}{x(x-1)} \quad (\sim 1/x^2 \quad \text{for } x \rightarrow \infty), \quad (29)$$

$$g_n(x) \stackrel{\text{def}}{=} \prod_{m=1}^n \frac{x + 2m - 1}{x - 2m} \equiv \frac{\Gamma(\frac{1}{2}x - n) \Gamma(\frac{1}{2}(x+1) + n)}{\Gamma(\frac{1}{2}x) \Gamma(\frac{1}{2}(x+1))} \quad (30)$$

$$\equiv g(x) (-1)^n \frac{\Gamma(\frac{1}{2}(x+1) + n)}{\Gamma(1 - \frac{1}{2}x + n)}, \quad g(x) \stackrel{\text{def}}{=} \frac{\sqrt{\pi} 2^{x-1}}{\sin(\pi x/2) \Gamma(x)} \quad (31)$$

(by the duplication and reflection formulae for  $\Gamma$ ). The resulting residues are

$$\operatorname{Res}_{x=1} f_n = -\frac{(-1)^n}{A_{n0}}, \quad \operatorname{Res}_{x=2m} f_n = (-1)^{n+m} A_{nm} \quad (m = 0, 1, 2, \dots),$$

with

$$A_{nm} = 2^{-2n} \frac{(n+m, n-m, 2m)!}{2m-1} \equiv \frac{1}{(2m-1)(n-m)!m!} \frac{\Gamma(n+m+1/2)}{\Gamma(m+1/2)}, \quad (32)$$

where  $(i, j, k)! \stackrel{\text{def}}{=} \frac{(i+j+k)!}{i!j!k!}$  (multinomial coefficient).

For later use, the partial fraction decomposition itself of  $f_n$  is

$$f_n(x) = (-1)^n \left[ \frac{-1}{A_{n0}} \frac{1}{x-1} + \sum_{m=0}^n \frac{(-1)^m A_{nm}}{x-2m} \right] : \quad (33)$$

enforcing  $f_n(x) \underset{x \rightarrow \infty}{\sim} 1/x^2$  from (29) upon the right-hand side first confirms the constant term therein to be 0 as shown, then yields two more identities:

$$\sum_{m=0}^n (-1)^m A_{nm} \equiv \frac{1}{A_{n0}}, \quad 2 \sum_{m=1}^n (-1)^m A_{nm} m \equiv (-1)^n + \frac{1}{A_{n0}}. \quad (34)$$

Next, for each  $n$  we select a contour  $\mathcal{C}_n$  that just encircles the real interval  $[1, 2n]$  positively (to encircle the subinterval  $[2, 2n]$  would suffice, but here it will always be beneficial to *dilate*, not shrink,  $\mathcal{C}_n$ ). Our final result is then

$$\Lambda_n \stackrel{\text{def}}{=} \frac{1}{2\pi i} \oint_{\mathcal{C}_n} f_n(x) \log 2\xi(x) dx \quad (\text{with } f_n \text{ from (29)}) \quad (35)$$

$$\equiv (-1)^n \sum_{m=1}^n (-1)^m A_{nm} \log 2\xi(2m), \quad n = 1, 2, \dots, \quad (36)$$

and the latter form is *fully explicit*:  $A_{nm}$  are given by (32), and

$$2\xi(2m) = \frac{(-1)^{m+1} B_{2m}}{(2m-3)!!} (2\pi)^m \equiv \frac{2(-1)^{m+1} B_{2m}}{\Gamma(m-\frac{1}{2})} \pi^{m+1/2}, \quad m = 0, 1, \dots \quad (37)$$

$$E.g., \Lambda_1 = \frac{3}{2} \log \frac{\pi}{3}, \quad \Lambda_2 = \frac{5}{24} \log \left[ \left( \frac{2}{5} \right)^7 \frac{3^{11}}{\pi^4} \right], \quad \Lambda_3 = \frac{21}{80} \log \left[ \frac{5^{25} \pi^8}{2^3 (3^2 \cdot 7)^{11}} \right]. \quad (38)$$

So, we deformed Keiper's  $\{\lambda_n^K\}$  by discretizing the derivatives on  $\log 2\xi$  to *finite differences* anchored at locations  $1, \{2m\}$  where  $\xi$  has known values, in a canonical way basically dictated by the *preservation of RH-sensitivity*.<sup>2</sup> This discretized Keiper sequence  $\{\Lambda_n\}$  has the *elementary closed form* (36), which is moreover directly computable at any  $n$  (in welcome contrast to the original  $\lambda_n$ , which need an iterative procedure all the way up from  $n = 1$ ).

---

<sup>2</sup>One still has the freedom to spread the  $x_m$  further out by skipping some locations ( $2j$ ), (or inversely, to keep some residual degeneracy if ever this were to ease computations).

## 2.2 Remarks.

1) Thanks to the second sum rule (34), the  $(\log 2\pi)$ -contributions to (36) from the first expression (37) can be summed, resulting in  $\Lambda_n \equiv \frac{1}{2} \log 2\pi + u_n$  with

$$u_n \stackrel{\text{def}}{=} (-1)^n \left[ \sum_{m=1}^n (-1)^m A_{nm} \log \frac{|B_{2m}|}{(2m-3)!!} + \frac{1}{2A_{n0}} \log 2\pi \right] : \quad (39)$$

this sequence  $\{u_n\}$  is the one used in our first note [34]. Likewise, the right-most expression (37) leads to the partially summed form

$$\Lambda_n \equiv \frac{1}{2} \log \pi + (-1)^n \left[ \sum_{m=1}^n (-1)^m A_{nm} \log \frac{|B_{2m}|}{\Gamma(m-\frac{1}{2})} + \left( \frac{1}{A_{n0}} - A_{n0} \right) \log 2 + \left( \frac{1}{A_{n0}} - \frac{A_{n0}}{2} \right) \log \pi \right], \quad (40)$$

suitable for computer routines able to directly deliver  $(\log \Gamma)$ .

2) If in place of (37) we evaluate  $\log 2\xi(2m)$  using (1) plus the expanded logarithm of the Euler product:  $\log \zeta(x) \equiv \sum_{p \text{ prime}} \sum_{r=1}^{\infty} \frac{p^{-rx}}{r}$ , then (36) gives an *arithmetic* form for  $\Lambda_n$ , like Bombieri–Lagarias’s Thm 2 for  $\lambda_n^L$ . [7, § 3]

3) Báez-Duarte [2] has an equally explicit sequential criterion for RH in terms of the  $B_{2m}$ , but in which the critical threshold is inordinately large,  $n \gtrsim e^{\pi T_0}$  [23, § 4] ([14, § 7] quotes  $n \gtrsim 10^{600,000,000}$ ); for our  $\Lambda_n$  the analogous  $n$ -value will prove considerably lower (§ 4.2).

4) The whole scheme will be extended from the Riemann zeta function  $\zeta$  to certain *Dirichlet L-functions* in § 3.5, then to some linear combinations thereof, specifically the *Davenport–Heilbronn* functions, in § 4.4.

## 2.3 Expression of $\Lambda_n$ in terms of the Riemann zeros

Let the primitive  $F_n$  of the function  $f_n$  in (29), (33) be defined by

$$\begin{aligned} F_n(x) &\stackrel{\text{def}}{=} \int_{\infty}^x f_n(y) dy && (\Rightarrow F_n(x) \sim -1/x \text{ for } x \rightarrow \infty) \\ &\equiv (-1)^n \left[ -\frac{1}{A_{n0}} \log(x-1) + \sum_{m=0}^n (-1)^m A_{nm} \log(x-2m) \right] \end{aligned} \quad (41)$$

and by single-valuedness in the whole  $x$ -plane minus the cut  $[0, 2n]$  : e.g.,  $F_1(x) = \frac{1}{2} \log [x(x-2)^3/(x-1)^4]$ .

Then in terms of (41), the  $\Lambda_n$  are expressible by summations over the zeros (which converge like  $\sum_{\rho} 1/\rho$  for any  $n$ , hence need the rule (3)):

$$\Lambda_n \equiv \sum_{\rho} F_n(\rho), \quad n = 1, 2, \dots \quad (42)$$

(In the original  $\lambda_n^K$ , (26) uses  $[x/(x-1)]^n$  in place of  $g_n(x)$ , which exceptionally yields *rational* functions  $n^{-1}[1 - (1 - 1/(1-x))^n]$  in place of the  $F_n(x)$ , for which (42) restores (7).)

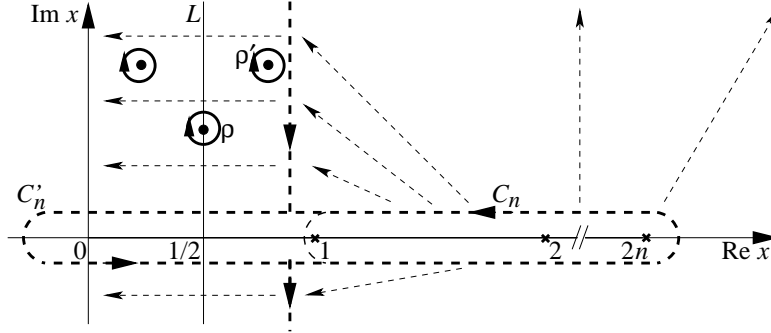


Figure 3: As Fig. 1 left, but superposing the deformation of the integration path for the integral (43) in which the function  $\xi'/\xi$  has the Riemann zeros as simple poles. A symmetrical lower half-plane is implied.

Proof of (42) (outlined, see fig. 3): first stretch the contour  $\mathcal{C}_n$  in (35) to  $\mathcal{C}'_n$  fully enclosing the cut  $[0, 2n]$  of  $F_n$  (as allowed by  $\log 2\xi(0) = 0$ ). Since  $F_n$  is single-valued on  $\mathcal{C}'_n$ , the so modified (35) can be integrated by parts,

$$\Lambda_n \stackrel{\text{def}}{=} -\frac{1}{2\pi i} \oint_{\mathcal{C}'_n} F_n(x) \left[ \frac{\xi'}{\xi} \right] (x) dx, \quad (43)$$

then the contour  $\mathcal{C}'_n$  can be further deformed into a sum of an outer anti-clockwise circle  $\mathcal{C}_R$  centered at  $\frac{1}{2}$  of radius  $R \rightarrow \infty$  (not drawn), and of small clockwise circles around the poles of the meromorphic function  $\xi'/\xi$  inside  $\mathcal{C}_R$ ; these poles are the Riemann zeros  $\rho$  therein, and each contributes  $F_n(\rho)$ . By the Functional Equation (1), the integral on  $\mathcal{C}_R$  is also  $\oint_{\mathcal{C}_R} \langle F_n(x) \rangle \left[ \frac{\xi'}{\xi} \right] (x) dx$ , where  $\langle F_n(x) \rangle \stackrel{\text{def}}{=} \frac{1}{2}[F_n(x) + F_n(1-x)] = O(1/x^2)$ ; then this integral tends

to 0 if  $R \rightarrow \infty$  while keeping at a distance from ordinates of Riemann zeros in a classic fashion (so that  $|\zeta'/\zeta|(r+iR) < K \log^2 R$  for all  $r \in [-1, +2]$ , cf. [10, p. 108]), hence (42) results.  $\square$

### 3 Resulting new sequential criterion for RH

Like the elusive Keiper–Li sequence, the fully explicit one  $\{\Lambda_n\}$  proves RH-sensitive (just slightly differently). The argument will use the function

$$\Phi(X) \stackrel{\text{def}}{=} X \log\left(1 - \frac{1}{X^2}\right) + \log \frac{X+1}{X-1} \equiv \int_{\infty}^X \log\left(1 - \frac{1}{Y^2}\right) dY \text{ on } \mathbb{C} \setminus [-1, 1]. \quad (44)$$

#### 3.1 Asymptotic criterion

Our main result is an *asymptotic* sensitivity to RH as  $n \rightarrow \infty$ , through this alternative for  $\{\Lambda_n\}$  which parallels (17)–(18) for  $\{\lambda_n\}$ :

- RH false:  $\Lambda_n \sim \sum_{\rho' - \frac{1}{2} \in 2n \mathcal{D}_{R_0}} F_n(\rho') \pmod{o(R^n) \forall R > R_0 > 1}, \quad (45)$

where  $\mathcal{D}_{R_0} \stackrel{\text{def}}{=} \{X \in \mathbb{C} \mid \text{Re } \Phi(X) > \log R_0\}$   
 $\subset \{\text{Re } X > 0\}$ , so the sum (45) is a truncation of  $\sum_{\text{Re } \rho' > \frac{1}{2}}$ ,

and  $F_n(\rho') \sim \frac{g(\rho')}{\rho'(\rho' - 1)} (-1)^n \frac{n^{\rho' - \frac{1}{2}}}{\log n} \quad (n \rightarrow \infty)$  for each given  $\rho'$  (46)

(giving a power-like growing oscillation *about* 0, cf. (31));

- RH true:  $\Lambda_n \sim \log n + C, \quad C = \frac{1}{2}(\gamma - \log \pi - 1) \approx -0.783757110474; \quad (47)$   
(implying asymptotic *positivity*);

a comparison with (24) yields  $C \equiv c + \frac{1}{2} \log 2$ , which testifies to a preserved kinship of  $\Lambda_n$  to  $\lambda_n^K$ .

For the RH false case, the pair (45)–(46) is formally, in the variable  $\log n$ , an expansion in exponentials multiplied by divergent power series (i.e., a *transseries*), to be interpreted with caveats as detailed in § 3.2.

The derivation scheme will transpose the arguments of § 1.3 to  $\Lambda_n$  expressed in an integral form and now in the  $x$ -plane: either (35) (using the

function  $g_n(x)$ ) in place of (20), or its integral by parts (43) (using  $F_n(x)$ ) in place of (21). Two new problems arise here: the large- $n$  forms of  $g_n(x)$  and  $F_n(x)$  need to be worked out, and the geometry of the integrands is strongly  $n$ -dependent hence the relative scales of  $n$  and  $x$  will matter.

- If we need *uniform* asymptotics in the integrands we must rescale the geometry as, for instance,  $x = \frac{1}{2} + 2nX$  : this condenses the singularities onto the fixed  $X$ -segment  $[0, 1]$  as  $n \rightarrow \infty$ . The Stirling formula applied to the ratio of  $\Gamma$  functions in (30) then yields

$$g_n(\frac{1}{2} + 2nX) \sim \left(\frac{X+1}{X-1}\right)^{1/4} e^{n\Phi(X)} \quad \text{for } n \rightarrow \infty, \quad (48)$$

with the function  $\Phi(X)$  from (44).

Next, integrating for  $F_n(x) = \int_{\infty}^x \frac{g_n(y)}{y(y-1)} dy$ , with  $y = \frac{1}{2} + 2nY$  yields

$$F_n(\frac{1}{2} + 2nX) \sim \frac{1}{2n} \int_{\infty}^X \frac{dY}{Y^2} \left(\frac{Y+1}{Y-1}\right)^{1/4} e^{n\Phi(Y)}, \quad (49)$$

which is a Laplace transform in the integration variable  $\Phi$ , hence it has an asymptotic power series in  $(1/n)$  (usually divergent) starting as [13, eq. 2.2(2)]

$$\begin{aligned} F_n(\frac{1}{2} + 2nX) &\sim \frac{1}{2n} \frac{1}{X^2} \left(\frac{X+1}{X-1}\right)^{1/4} \frac{e^{n\Phi(X)}}{n\Phi'(X)} \\ &= \frac{1}{2n^2} \frac{1}{X^2} \left(\frac{X+1}{X-1}\right)^{1/4} \frac{e^{n\Phi(X)}}{\log(1-1/X^2)} \end{aligned} \quad (50)$$

- Whereas if we let  $n \rightarrow \infty$  at *fixed*  $x$ , (31) at once implies

$$g_n(x) \sim g(x)(-1)^n n^{x-1/2} \sim g(x)(-1)^n e^{\log n(x-1/2)}. \quad (51)$$

Here  $(\log n)$  occupies the place of  $n$  as large parameter, and the same Laplace argument for the integral  $F_n(x) = \int_{\infty}^x \frac{g_n(y)}{y(y-1)} dy$  now yields an asymptotic series in powers of  $(1/\log n)$  (usually divergent), starting as

$$F_n(x) \sim \frac{g(x)}{x(x-1)} (-1)^n \frac{n^{x-1/2}}{\log n}. \quad (52)$$

### 3.2 Details for the case RH false

As in § 1.3.1, we can apply the steepest-descent method to the integral (43) written in the global variable  $X$ . We rescale the contour  $C'_n$  then deform it toward level contours  $\text{Re } \Phi(X) = \Phi_0 \rightarrow 0^+$ : these approach the completed critical line in the  $X$ -plane,  $\{\text{Re } X = 0\} \cup \{\infty\}$ , from the  $\{\text{Re } X > 0\}$  side (fig. 4). Apart from staying on this side (and being rescaled to the  $X$ -plane), the contour deformation is isotopic to that used in § 2.3, hence it likewise yields a contribution  $F_n(\rho')$  per RH-violating zero  $\rho'$  whose rescaled image  $X_{\rho'} \equiv (\rho' - \frac{1}{2})/(2n)$  has  $\text{Re } \Phi(X_{\rho'}) > \Phi_0 > 0$ ; i.e., overall,

$$\sum_{\text{Re } \Phi(X_{\rho'}) > \Phi_0} F_n(\rho').$$

(The novelty vs (42) is that now the terms come asymptotically ordered.) For  $X \rightarrow \infty$ ,  $\Phi(X) \sim 1/X$ , hence the level curves asymptotically become  $\{\text{Re}(1/X) = \Phi_0\}$  (circles tangent to the imaginary  $X$ -axis at 0). Thus the above sum over zeros has a natural cutoff  $|\text{Im } \rho'| \lesssim \sqrt{n/\Phi_0}$ , which is the height above which the disk  $\{\text{Re}(1/X) > \Phi_0\}$  parts from the critical strip.

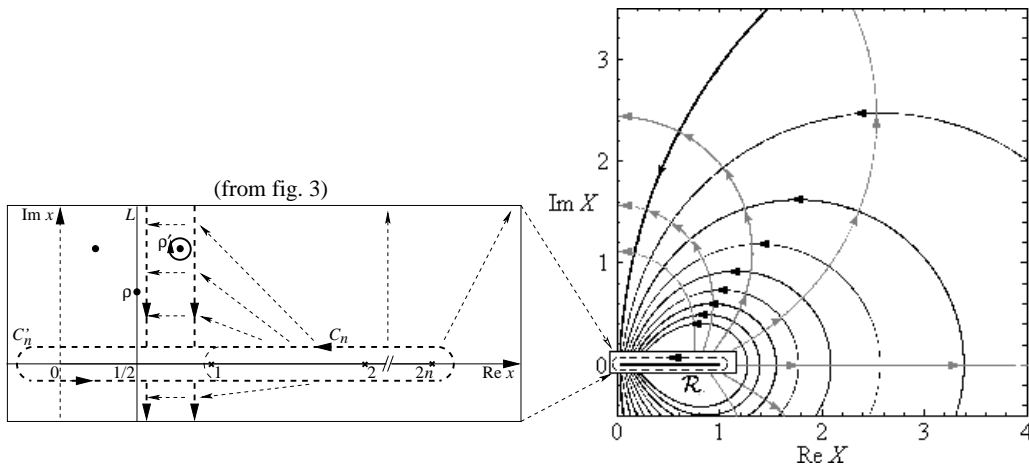


Figure 4: (at right) as fig. 3 but using the global variable  $X \stackrel{\text{def}}{=} (x - \frac{1}{2})/(2n)$  in the integral (43) (fig. 3 now fills the rectangle  $\mathcal{R}$ ). Mathematica [35] contour plots for  $\Phi(X)$  of (44): in black, deformed integration contours (level curves  $\{\text{Re } \Phi(X) = \Phi_0\}$ ,  $\Phi_0 \downarrow 0^+$ ); in gray, steepest-descent lines (level curves of  $\text{Im } \Phi$ ).

When zooming in to the  $n \rightarrow \infty$ , fixed- $x$  regime, then by (52) the level curves turn to parallel lines  $\{\text{Re } x - \frac{1}{2} = t_0\}$ , and the deformation to  $t_0 \rightarrow 0^+$

(fig. 4 left). Only a portion of contour  $\mathcal{C}'_n \cap \{\operatorname{Re} x - \frac{1}{2} < \varepsilon\}$  escapes the deformation, but by (52) its contribution to the integral (43) is  $O(n^\varepsilon)$ , ultimately negligible. Therefore,  $\Lambda_n \pmod{o(R^n)} \forall R > e^{\Phi_0}$  equals the above sum  $\sum_{\rho'} F_n(\rho')$ , which proves (45) under the replacement  $R_0 = e^{\Phi_0}$ .

This fixed- $x$  regime actually governs *each individual term* of the sum (45), since any given zero lives at fixed  $x$ : thus, setting  $x = \rho'$  in (52) directly yields the asymptotic form (46) which is *explicit* including the  $n$ -dependence, unlike the  $F_n(\rho')$  for  $n \rightarrow \infty$ . Now the sum (45) as a whole cannot be reexpressed that way, because (46) is not uniform in  $x$ ; and indeed, a closed asymptotic form for  $\Lambda_n$  is out of reach: just as for  $\lambda_n$  in § 1.3.2 it would encode the asymptotic distribution of the Riemann zeros, but this stays fundamentally undetermined (because *truly 2-dimensional*) if RH is false. Still, (46) correctly specifies the contribution to  $\Lambda_n$  from *any single* RH-violating zero  $\rho' \equiv \frac{1}{2} + t + iT$  ( $t > 0$ ): i.e., a term *cycling around zero* of amplitude *growing with  $n$*  as

$$|F_n(\rho')| \approx \frac{1}{T^2 \log n} \left( \frac{2n}{|T|} \right)^t \quad \text{for } n \gg |T| \quad (53)$$

(upon using  $|g(\rho')| \approx (2/|T|)^t$  for  $|T| > T_0 \gg 1$ ).

If now RH is true then, as  $\Phi_0$  attains  $0^+$ , (45) reaches no better than  $\Lambda_n = o(R^n)$  ( $\forall R > 1$ ), and only a finer analysis of the limiting integral on the critical line  $L$  will lead to a definite asymptotic form, as follows.

### 3.3 Details for the case RH true

Here our quickest path is to adapt Oesterlé's argument from §1.3.2.

To deform  $\{\lambda_n\}$  to  $\{\Lambda_n\}$ , we replaced  $\left(\frac{x}{x-1}\right)^n$  in (26) by  $g_n(x)$  from (30). That changes (22) to

$$\Lambda_n = \int_0^\pi 2 \sin \Theta_n(\theta) N\left(\frac{1}{2} \cot\left(\frac{1}{2}\theta\right)\right) d\theta, \quad (54)$$

where  $\Theta_n \in (0, n\pi]$  (previously for  $\lambda_n : \Theta_n \equiv n\theta$ ) is now the sum of the  $n$  angles subtended by the real vectors  $(\overline{1-2m}, \overline{2m})$  from the point  $\frac{1}{2} + iT$ , for  $m = 1, 2, \dots, n$ . The two *endpoint slopes* of the function  $\Theta_n(\theta)$  will then play the main (independent) roles:

$$\Theta'_n(0) = \sum_{m=1}^n (4m-1) \equiv n(2n+1), \quad (55)$$

$$\Theta'_n(\pi) = \sum_{m=1}^n (4m-1)^{-1} \equiv \frac{1}{4}[(\Gamma'/\Gamma)(n + \frac{3}{4}) + \gamma + 3 \log 2 - \pi/2]. \quad (56)$$

We then follow the same steps as with  $\lambda_n^K$  in § 1.3.2.

1)  $\int_0^\pi 2 \sin \Theta_n(\theta) \delta N(\frac{1}{2} \cot(\frac{1}{2}\theta)) d\theta = o(1)$  if a nonstationary-phase principle applies for the oscillatory function  $\sin \Theta_n(\theta)$ , i.e., the minimum slope of  $\Theta_n(\theta)$  ( $\theta \in [0, \pi]$ ) must go to  $\infty$  with  $n$ : previously (with  $\Theta_n \equiv n\theta$ ) that slope was  $n$ , now it is  $\Theta'_n(\pi) \sim \frac{1}{4} \log n$  which still diverges for  $n \rightarrow \infty$  therefore gives that  $o(1)$  bound (but due to  $\Theta'_n(\pi) \ll n$ , this  $o(1)$  might decay much more slowly than the corresponding  $o(1)$  for  $\lambda_n^K$ ).

2) In this step (i.e.,  $T \rightarrow +\infty$ ), only  $\theta \rightarrow 0$  behaviors enter; here  $\Theta_n(\theta) \sim \Theta'_n(0)\theta$ , vs  $n\theta$  previously, so it suffices to substitute  $\Theta'_n(0)$  for  $n$  in the asymptotic result (24) for  $\lambda_n^K$ , to get

$$\Lambda_n \sim \frac{1}{2} \log \Theta'_n(0) + c = \frac{1}{2} \log[n(2n+1)] + c \sim \log n + (c + \frac{1}{2} \log 2). \quad (57)$$

□

### 3.4 Asymptotic or full-fledged Li's criterion for $\{\Lambda_n\}$ ?

(a heuristic parenthesis).

A full Li's criterion for the new sequence  $\{\Lambda_n\}$  would read as

$$\text{RH} \iff \Lambda_n > 0 \text{ for all } n \quad (\text{unproven})$$

but anyway, such a forcible inclusion of *all*  $n$  is not vital in our focus on RH-sensitivity: already for the  $\lambda_n$ , only the  $n \gg 1$  region counted (§ 1.2); and likewise, our criterion (45)–(47) entails  $\Lambda_n > 0$  *asymptotically* if and only if RH holds (fig. 9 will illustrate that on a counterexample to RH).

As for low  $n$ ,  $\Lambda_n > 0$  will prove *numerically* manifest there (see § 4.1).

All those observations make us *conjecture* that Li's criterion fully holds for the sequence  $\{\Lambda_n\}$  as well (but appears harder to prove than for  $\{\lambda_n\}$ ).

### 3.5 Generalized-RH asymptotic alternative

All previous developments carry over from  $\zeta(x)$  to *Dirichlet L-functions*, which have the form (using the Hurwitz zeta function  $\zeta(x, w)$ )

$$L_\chi(x) \stackrel{\text{def}}{=} \sum_{k=1}^{\infty} \frac{\chi(k)}{k^x} \equiv d^{-x} \sum_{k=1}^d \chi(k) \zeta(x, k/d), \quad (58)$$

where  $\chi$  is a special type of  $d$ -periodic function on  $\mathbb{Z}$  ( $d > 1$ ): a *real primitive Dirichlet character* (which then has a definite parity, even or odd). [10, chaps. 5–6] Such  $L_\chi(x)$  have very close properties to Riemann's  $\zeta(x)$  :

- Functional equations: [10, chap. 9]

$$\xi_\chi(x) \stackrel{\text{def}}{=} (\pi/d)^{-x/2} \Gamma(\frac{1}{2}(x+b)) L_\chi(x) \equiv \xi_\chi(1-x), \quad b = \begin{cases} 0 & (\chi \text{ even}) \\ 1 & (\chi \text{ odd}) \end{cases}. \quad (59)$$

- Explicit values at integers, in terms of Bernoulli polynomials: by the classic identities  $(\ell+1)\zeta(-\ell, a) = -B_{\ell+1}(a)$  ( $\ell = 0, 1, 2, \dots$ ), (58) makes  $L_\chi(x)$  explicit at all  $x = -\ell$ ; the functional equation (59) then converts that to explicit values for  $L_\chi$  (and  $\xi_\chi$ ) at all *even, resp. odd, positive integers* according to the *even, resp. odd* parity of  $\chi$ . And  $L_\chi(1)$  (hence  $\xi_\chi(1)$ ) is explicitly computable also for even parity. [10, chap. 1][32, eq.(10.70)]

- Generalized Riemann Hypothesis (GRH): *all* zeros  $\rho$  of  $\xi_\chi$  have  $\text{Re } \rho = \frac{1}{2}$ .
- A Keiper–Li sequence  $\lambda_{\chi,n}$  exists for  $\xi_\chi$  in full similarity to the case of Riemann's  $\xi$ . For GRH, the only change in our asymptotic alternative (17)–(18) affects the constant  $c$  in (18) or (24) due to the replacement, in the asymptotics of the counting function  $N(T)$  as used in § 1.3.2, of the term  $\log(T/2\pi)$  by  $\log(Td/2\pi)$ , [10, chap. 16] which results in

$$\text{GRH true: } \lambda_{\chi,n}^K \sim \frac{1}{2} \log n + c_d \pmod{o(1)}, \quad c_d = c + \frac{1}{2} \log d. \quad (60)$$

Then as before, the definition of  $\{\lambda_{\chi,n}^K\}$  can be discretized to yield an explicit sequence  $\{\Lambda_{\chi,n}\}$  involving finite differences of *elementary*  $\log \xi_\chi$ -values. For even  $\chi$ , everything stays as in § 2.1 (where even parity is implied throughout), hence  $\Lambda_{\chi,n}$  are given by (36) with  $2\xi(2m)$  simply replaced by  $\frac{1}{\xi_\chi(1)} \xi_\chi(2m)$ . For odd  $\chi$  on the other hand, the points  $x_m$  have to be relocated from  $2m$  to  $2m+1$ , resulting in these main changes:

$$\begin{aligned} [(31) \rightarrow] \quad g_n^{\text{odd}}(x) &\stackrel{\text{def}}{=} \prod_{m=1}^n \frac{x+2m}{x-2m-1} \equiv g^{\text{odd}}(x) (-1)^n \frac{\Gamma(\frac{1}{2}x+1+n)}{\Gamma(\frac{1}{2}(3-x)+n)}, \\ &g^{\text{odd}}(x) \stackrel{\text{def}}{=} \frac{-\sqrt{\pi} 2^{x-1}}{\cos(\pi x/2) \Gamma(x)}, \end{aligned} \quad (61)$$

$$[(32) \rightarrow] \quad A_{nm}^{\text{odd}} = 2^{-2n} (n+m, n-m, 2m+1)! / (2m+1), \quad (62)$$

$$[(41) \rightarrow] \quad F_n^{\text{odd}}(x) = (-1)^n \left[ \frac{-1}{A_{n0}^{\text{odd}}} \log x + \sum_{m=0}^n (-1)^m A_{nm}^{\text{odd}} \log(x-2m-1) \right], \quad (63)$$

$$[(36) \rightarrow] \quad \Lambda_{\chi,n} \equiv (-1)^n \sum_{m=1}^n (-1)^m A_{nm}^{\text{odd}} \log \left[ \frac{1}{\xi_{\chi}(1)} \xi_{\chi}(2m+1) \right] \quad (\chi \text{ odd}). \quad (64)$$

All in all, the asymptotic alternative (45)–(47) generalizes to one depending on  $\chi$ , via its parity on the “false” side, and period  $d$  on the “true” side:

- GRH false:  $\Lambda_{\chi,n} \sim \sum_{\rho' - \frac{1}{2} \in 2n \mathcal{D}_{R_0}} F_n^{\#}(\rho') \pmod{o(R^n) \forall R > R_0 > 1}$  (65)

and, for each given GRH-violating zero  $\rho'$ ,

$$F_n^{\#}(\rho') \sim \frac{g^{\#}(\rho')}{\rho'(\rho' - 1)} (-1)^n \frac{n^{\rho' - \frac{1}{2}}}{\log n} \quad (n \rightarrow \infty), \quad (66)$$

$$\text{with } (F_n^{\#}, g^{\#}) \stackrel{\text{def}}{=} \begin{cases} (F_n, g) & \text{for } \chi \text{ even, cf. (41), (31)} \\ (F_n^{\text{odd}}, g^{\text{odd}}) & \text{for } \chi \text{ odd, cf. (63), (61)} \end{cases}; \quad (67)$$

- GRH true:  $\Lambda_{\chi,n} \sim \log n + C_d \pmod{o(1)}$ ,  $C_d = C + \frac{1}{2} \log d$  (68)

( $\equiv c_d + \frac{1}{2} \log 2$ ), cf. (47), (60).

## 4 Quantitative aspects

We now discuss how the discretized Keiper sequence  $\{\Lambda_n\}$  vs the Keiper–Li  $\{\lambda_n\}$  might serve as a *practical* probe for RH in a complementary perspective to standard tests. (To rigorously (dis)prove RH using  $\{\Lambda_n\}$  is also a prospect in theory, but we have not worked on that.)

### 4.1 Numerical data in the Riemann case

Low- $n$  calculations of  $\Lambda_n$  (fig. 5) agree very early with the *RH-true* behavior (here, (47)), just as was the case for  $\lambda_n$  [18][21]. The remainder term  $\delta\Lambda_n \stackrel{\text{def}}{=} \Lambda_n - (\log n + C)$  looks compatible with an  $o(1)$  bound (fig. 6), albeit less neatly than the analogous  $\delta\lambda_n^K$  [18, fig. 1][21, fig. 6b], (note: even Keiper [18] plotted  $\delta\lambda_n^L = n \delta\lambda_n^K$ ). For the record,

$$\begin{aligned} \Lambda_1 &\approx 0.069176395771, \quad \Lambda_2 \approx 0.22745427267, \quad \Lambda_3 \approx 0.45671413349; \quad (\text{cf. (38)}) \\ n = 2000 : \quad \Lambda_n &\approx 6.815360445451163 \quad (\delta\Lambda_n \approx -0.0017849), \end{aligned}$$

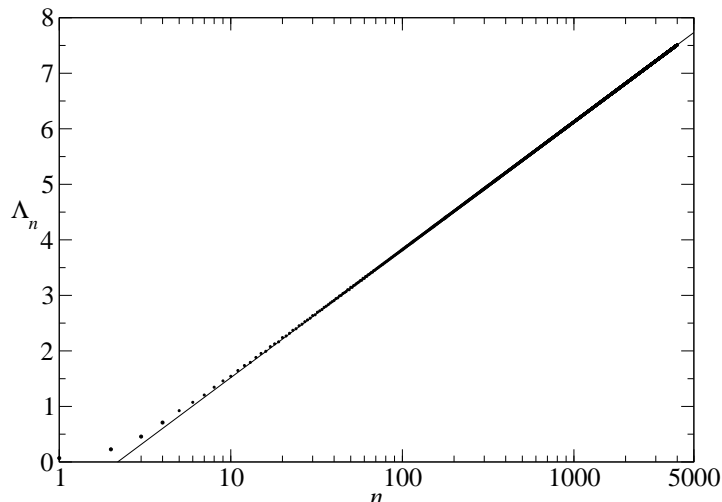


Figure 5: The coefficients  $\Lambda_n$  computed by (36) up to  $n = 4000$ , on a logarithmic  $n$ -scale (straight line: the RH-true form  $(\log n + C)$  of (47)).

$$\begin{aligned}
 n = 10000 : \quad & \Lambda_n \approx 8.428662659671506 \quad (\delta\Lambda_n \approx +0.0020794), \\
 n = 20000 : \quad & \Lambda_n \approx 9.119244876955247 \quad (\delta\Lambda_n \approx -0.000485565), \\
 n = 100000 : \quad & \Lambda_n \approx 10.729678153023 \quad (\delta\Lambda_n \approx +0.0005097985), \\
 n = 200000 : \quad & \Lambda_n \approx 11.42244991847 \quad (\delta\Lambda_n \approx +0.0001343834) \\
 n = 500000 : \quad & \Lambda_n \approx 12.33812102688 \quad (\delta\Lambda_n \approx -0.0004852401)
 \end{aligned} \tag{69}$$

( $n > 20000$  samples: courtesy of G. Misguich, [24] see § 4.5).

The main oscillation in  $(-1)^n \delta\Lambda_n$  (fig. 6) must come from  $F_n(\rho_1)$  in (42) for the lowest Riemann zero  $\rho_1$ : the  $(\log n)$ -period agrees with  $2\pi/\text{Im } \rho_1$  (per the asymptotic form (52)), as  $2\pi/14.1347 \approx 0.44$ .

## 4.2 Imprints of putative zeros violating RH

RH-violating zeros  $\rho'$  (if any) seem to enter the picture just as for the  $\lambda_n$ : their contributions (46) will asymptotically dominate  $\log n$ , but numerically they will emerge and take over extremely late. Indeed for such a zero  $\rho' = \frac{1}{2} + t + iT$ , with  $0 < t < \frac{1}{2}$  and  $T \gtrsim 2.4 \cdot 10^{12}$  [15], its contribution scales like  $T^{-2}(2n/T)^t/\log n$  in modulus, by (53). We then get its crossover threshold (in order of magnitude, neglecting logarithms and constants against powers)

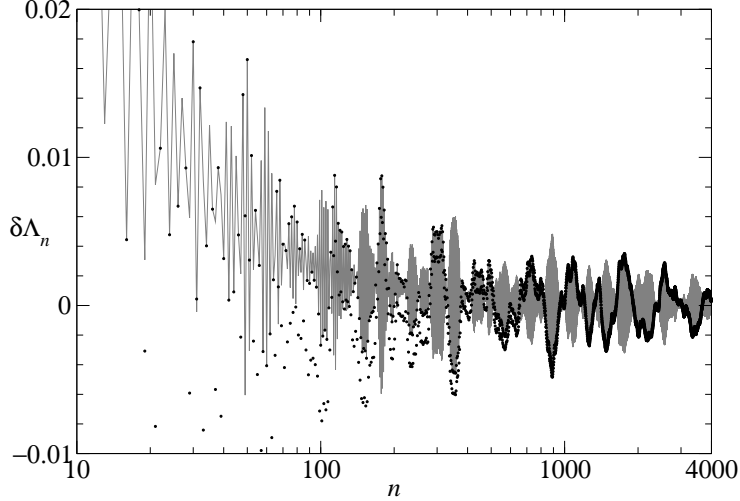


Figure 6: The remainder sequence  $\delta\Lambda_n = \Lambda_n - (\log n + C)$  (in gray: the connecting segments are drawn as visual cues only), and a rectified form  $(-1)^n \delta\Lambda_n$  (black dots) to cancel the period-2 oscillations.

by solving

$$T^{-2}(n/T)^t \approx 1 \quad (70)$$

$$\implies n \gtrsim T^{1+2/t} \quad (\text{best case: } O(T^{5+0}) \text{ for } t = \frac{1}{2} - 0). \quad (71)$$

This is worse than (19) for  $\lambda_n$ , all the more if  $\Lambda_n < 0$  were sought (the right-hand side of (70) should then be  $\log^2 n$ ). There is however room for possible improvement: the core problem is to filter out a weak  $\rho'$ -signal from the given background (47), therefore any predictable structure in the latter is liable to boost the gain. For instance, the hyperfine structure of  $\delta\Lambda_n$  is oscillatory of period 2 (fig. 6); this suggests to average over that period, which *empirically* discloses a rather neat  $(1/n)$ -decay trend (fig. 7):

$$\overline{\delta\Lambda_n} \stackrel{\text{def}}{=} \frac{1}{2}(\delta\Lambda_n + \delta\Lambda_{n-1}) \approx 0.25/n. \quad (72)$$

The same operation on a  $\rho'$ -signal  $F_n(\rho')$  in (45) roughly applies  $\frac{1}{2}(d/dn)$  to the factor  $n^T$  therein (again neglecting  $t \ll T$  and  $\log n$ ), i.e., multiplies it by  $\frac{1}{2}(T/n)$ . Thus heuristically, i.e., conjecturing the truth of (72) for  $n \rightarrow \infty$  under RH, the crossover condition improves from (70) to

$$\begin{aligned} (T/n) T^{-2}(n/T)^t &\approx \overline{\delta\Lambda_n} \approx 1/n \\ \implies n &\gtrsim T^{1+1/t} \quad (\text{best case: } O(T^{3+0}) \text{ for } t = \frac{1}{2} - 0). \end{aligned} \quad (73)$$

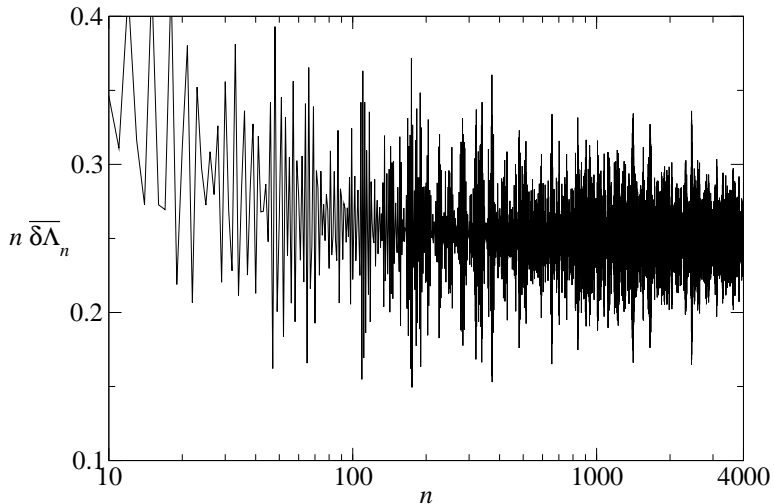


Figure 7: The averaged remainder sequence (72) rescaled by  $n$ , namely:  $n \overline{\delta\Lambda}_n$ . (Some further values: 0.27027 for  $n = 10000$ , 0.23970 for  $n = 20000$ , 0.2559 for  $n = 100000$ , 0.2683 for  $n = 200000$ , 0.27957 for  $n = 500000$ . [24])

We can hope that efficient signal-analysis techniques may still lower this detection threshold. Even an empirical mindset may be acceptable there: the  $\{\Lambda_n\}$  (like  $\{\lambda_n\}$ ) should anyway work best for *global coarse detection* of a possible RH-violation; this could then guide the classic algorithms [15] (which are local) to concentrate on a smaller region, and then confirm (or disprove) that RH-violating zero in full rigor.

### 4.3 The uncertainty principle for $\{\Lambda_n\}$

An absolute detection limit is however provided by the *uncertainty principle*, and this has to be quantified here. Near the critical line  $\{\text{Re } X = 0\}$  and for large  $n$ ,  $\Lambda_n$  is an integral of the zeros' distribution against essentially  $e^{n\Phi(i\text{Im } X)}$  (by (43), (50)), which is a distorted plane wave. To resolve  $t > 0$  for a zero  $\rho' = \frac{1}{2} + t + iT \equiv \frac{1}{2} + 2nX$ , the uncertainty principle asks its scale ( $\text{Re } X = t/(2n)$  in the  $X$ -plane) to be at least of the order of the local wavelength which is  $1/[n \log(1 + 1/(\text{Im } X)^2)]$  by (44), with  $\text{Im } X = T/(2n)$ : that means  $\frac{1}{2}t \log(1 + 4n^2/T^2) \gtrsim 1$  or, to a fair approximation when  $t < \frac{1}{2}$ ,

$$n \gtrsim \frac{1}{2}|T| e^{1/t}. \quad (74)$$

Against the corresponding bound  $n \gtrsim T^2/t$  for  $\{\lambda_n\}$  in § 1.2, at any given  $t > 0$  this will favor  $\{\Lambda_n\}$  once  $|T| \gtrsim \frac{1}{2}t e^{1/t}$ . E.g., at the current floor height (4), the best possible  $n$ -threshold (i.e., for  $t = \frac{1}{2} - 0$ ) gets improved to  $10^{13}$ , from  $10^{25}$  for  $\{\lambda_n\}$  in (19). That bound also allows for  $n$  to go well below the detection thresholds (71), (73) - *in principle*: there still remains to actually extract a putative  $\rho'$ -signal, extremely weak at such decreased  $n$ , from the “noise” created by the many more zeros lying nearby on the critical line.

#### 4.4 The Davenport–Heilbronn counterexamples

More tests of interest lie in the generalized setting of § 3.5 for *odd parity*. As Dirichlet L-function we only tested the  $\beta$ -function (of period 4) and saw no difference of behavior patterns in  $\{\Lambda_{\beta,n}\}$  vs  $\{\Lambda_n\}$ . If we then go beyond, there exist special periodic odd Dirichlet series that are *not* Dirichlet L-functions, but obey similar functional equations *and* have many zeros *off* the critical line  $L$ . [11][30, § 10.25][29][3][6, § 5] We may then seek a testing ground for the *RH-false branch* of our asymptotic alternative (generalized, as (65)–(66)).

Specifically, for  $\phi = \frac{1}{2}(1 + \sqrt{5})$  (the golden ratio), let

$$\tau_{\pm} \stackrel{\text{def}}{=} -\phi \pm \sqrt{1 + \phi^2} \quad (\tau_+ \approx 0.28407904384, \quad \tau_- = -1/\tau_+ \approx -3.52014702134); \quad (75)$$

$$\nu_{\pm}(k) \stackrel{\text{def}}{=} \{1, +\tau_{\pm}, -\tau_{\pm}, -1, 0, \dots\}_{k=1,2,\dots} \quad \text{periodically continued}$$

(an *odd* function on the integers mod 5); and, similarly to (58),

$$f_{\pm}(x) \stackrel{\text{def}}{=} \sum_{k=1}^{\infty} \frac{\nu_{\pm}(k)}{k^x} \equiv 5^{-x} \left\{ \zeta\left(x, \frac{1}{5}\right) + \tau_{\pm} \left[ \zeta\left(x, \frac{2}{5}\right) - \zeta\left(x, \frac{3}{5}\right) \right] - \zeta\left(x, \frac{4}{5}\right) \right\}. \quad (76)$$

These *Davenport–Heilbronn* (DH) functions  $f_{\pm}$  (denoted  $f_{\frac{1}{2}}$  in [3],  $f(\cdot; \tau_{\pm})$  in [6]) obey *the functional equation of odd Dirichlet L-functions*, namely (59) with  $b = 1$  and the period  $d = 5$ , up to a  $(\pm)$  sign: [3][6, § 5]

$$\xi_{\pm}(x) \stackrel{\text{def}}{=} (\pi/5)^{-x/2} \Gamma\left[\frac{1}{2}(1+x)\right] f_{\pm}(x) \equiv \pm \xi_{\pm}(1-x). \quad (77)$$

As in § 3.5, this makes  $f_{\pm}$ ,  $\xi_{\pm}$  *explicit* at the positive *odd* integers:

$$\xi_{\pm}(2m+1) = \mp \frac{2(-1)^m}{(2m+1)!!} \left[ B_{2m+1}\left(\frac{1}{5}\right) + \tau_{\pm} B_{2m+1}\left(\frac{2}{5}\right) \right] \sqrt{\pi} (10\pi)^m; \quad (78)$$

$$\text{e.g.,} \quad \xi_{\pm}(1) = \pm \frac{1}{5}(3 + \tau_{\pm})\sqrt{\pi} \quad \left\{ \begin{array}{l} \xi_+(1) \approx 1.1641757096 \\ \xi_-(1) \approx 0.1843873182 \end{array} \right\}$$

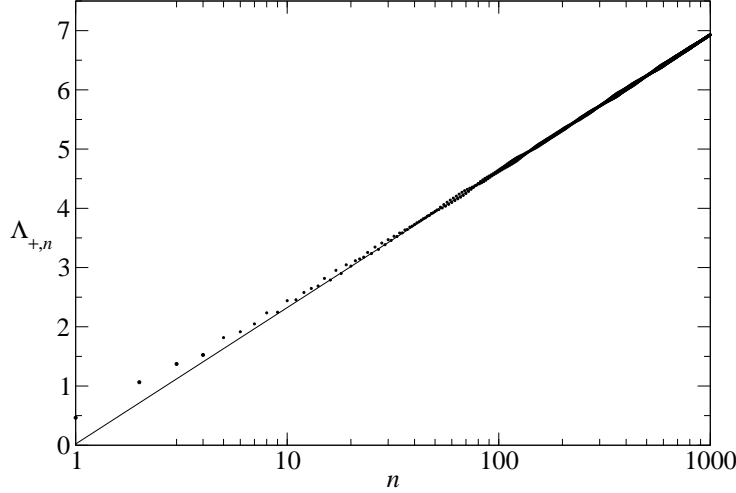


Figure 8: As fig. 5, but for the  $\Lambda_{+,n}$  of the Davenport–Heilbronn (DH) function  $f_+$  as given by (79), up to  $n = 1000$ ; e.g.,  $\Lambda_{+,1} \approx 0.4653858106$ ,  $\Lambda_{+,2} \approx 1.063986745$ . Straight line: the GRH-true form  $(\log n + C_5)$  of (80).

(we also used  $B_{2m+1}(1-a) \equiv -B_{2m+1}(a)$ ). So, in line with (64) we take

$$\Lambda_{\pm,n} \stackrel{\text{def}}{=} (-1)^n \sum_{m=1}^n (-1)^m A_{mn}^{\text{odd}} \log \left[ \frac{1}{\xi_{\pm}(1)} \xi_{\pm}(2m+1) \right] \quad (79)$$

as explicit sequences to probe our asymptotic criterion for GRH (as (65)–(68) with  $\# = \text{odd}$  and  $d = 5$ ) upon the DH functions  $f_{\pm}$  respectively (as cases with zeros off the critical line  $L$ ).

Now the numerics break the formal  $(\pm)$ -symmetry to a surprising extent.

For  $\xi_+$ , the lowest- $T$  zero off the line  $L$  is  $\rho'_+ \approx 0.808517 + 85.699348 i$ . [29] Then, for its detection through the sequence  $\{\Lambda_{+,n}\}$ , our predicted threshold (70) gives  $n \approx T^{1+2/t} \approx (85.7)^{7.48} \approx 3 \cdot 10^{14}$ : indeed, our low- $n$  data (fig. 8) solely reflect the GRH-true pattern (68) for  $d = 5$ ,

$$\Lambda_{+,n} \approx \log n + C_5, \quad C_5 = C + \frac{1}{2} \log 5 \approx +0.020961845743. \quad (80)$$

Whereas for  $\xi_-$ , the lowest- $T$  zero off  $L$  is  $\rho'_- \approx 2.30862 + 8.91836 i$ . [3] (Notations therein:  $\xi \equiv \tau_+$ ,  $f_2 \equiv f_-$ .) Now, not only is this zero well detached from the next higher one ( $\approx 1.94374 + 18.8994 i$ ), but above all it gives a detection threshold  $n \approx T^{1+2/t} \approx (8.92)^{2.11} \approx 100$ , extremely low!

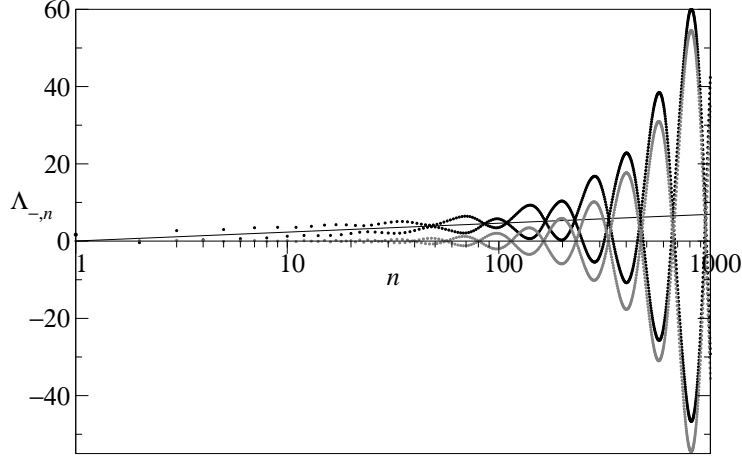


Figure 9: As fig. 8, but for the  $\Lambda_{-,n}$  of the DH function  $f_-$  (vertical scale shrunk); e.g.,  $\Lambda_{-,1} \approx 1.661697636$ ,  $\Lambda_{-,2} \approx -0.3913729841$  (already  $< 0$ ). Straight line: the GRH-true form  $(\log n + C_5)$  as in fig. 8; gray dots: the leading GRH-false form  $2 \operatorname{Re} F_n^{\text{odd}}(\rho'_-)$  from (63), (81), with  $\rho'_- \approx 2.30862 + 8.91836 i$ .

Indeed, fig. 9 shows a neat crossover of  $\Lambda_{-,n}$  from the GRH-true pattern (80) at low  $n$ , toward the dominant GRH-false pattern (65) at higher  $n$ , namely

$$F_n^{\text{odd}}(\rho'_-) + F_n^{\text{odd}}(\rho'^*_-) \equiv 2 \operatorname{Re} F_n^{\text{odd}}(\rho'_-). \quad (81)$$

Even though the form (80) is superseded by (81) asymptotically, its numerical contribution to  $\Lambda_{-,n}$  fully remains, hence to test (81) we first have to subtract (80) from  $\Lambda_{-,n}$ ; then, the remainder

$$\delta\Lambda_{-,n} \stackrel{\text{def}}{=} \Lambda_{-,n} - (\log n + C_5) \quad (82)$$

shows period-2 oscillations symmetrical about 0, so we rather plot  $(-1)^n \delta\Lambda_{-,n}$ : now fig. 10 shows that this is very well fitted by  $(-1)^n 2 \operatorname{Re} F_n^{\text{odd}}(\rho'_-)$  from (81). In turn, (66) specifies the latter explicitly to first order in  $(1/\log n)$ , and this also reasonably fits the data (with  $(1/\log n)$  not being that small).

Thus, numerical data for the sequences  $\{\Lambda_{\pm,n}\}$  support our asymptotic alternative in full. We stress that fig. 9 models how, at some much higher  $n$ ,  $\{\Lambda_n\}$  itself *will* blow up if RH (for  $\zeta(x)$ ) is false. The  $\Lambda_{\pm,n}$  also ought to be a testing ground for any ideas to detect RH false earlier with the  $\Lambda_n$ .

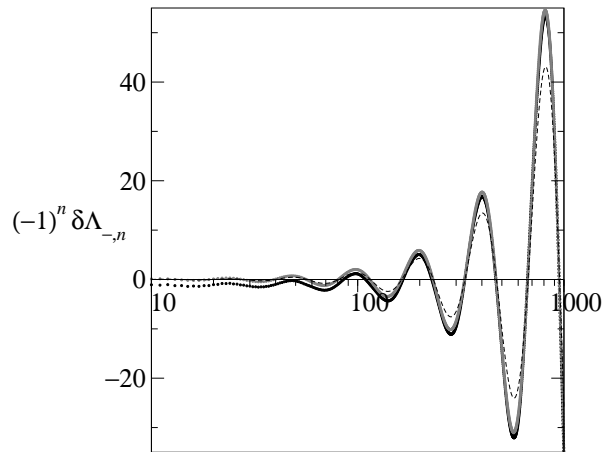


Figure 10: Asymptotics of the deviation (82) from GRH in the case of the DH function  $f_-$ . Black dots: the rectified remainder sequence  $(-1)^n \delta \Lambda_{-n}$ . Gray dots: the rectified asymptotic form  $(-1)^n 2 \operatorname{Re} F_n^{\text{odd}}(\rho'_-)$  from (81). Dashed curve: its large- $(\log n)$  explicit form  $2 \operatorname{Re} \left[ \frac{g^{\text{odd}}(\rho'_-)}{\rho'_-(\rho'_--1)} n^{\rho'_--1/2} \right] (\log n)^{-1}$  from (61), (66).

## 4.5 The hitch

We now refocus on the numerical quest for  $\{\Lambda_n\}$  (the Riemann case), to discuss a major issue. The  $(\log n)$ -sized values  $\Lambda_n$  result from alternating summations like (36) over terms growing *much faster* (exponentially) with  $n$ : very deep cancellations must then take place, which may explain the sensitivity of  $\Lambda_n$  (to RH) but also create a computational hurdle for  $n \gg 1$ , namely a loss of precision growing linearly with  $n$ . For sums like (36),  $\sum s_m$  of order comparable to unity, the *slightest* end accuracy requires each summand  $s_m$  to be input with a “base” precision  $\approx \log_{10} |s_m|$  (working in decimal digits throughout); plus uniformly adding  $D$  to reach  $\sum s_m$  accurate to  $D$  digits.

We can tune the required precision in (36) for each  $m$ -value at large given  $n$  by using the Stirling formula, to find that  $m_* \approx n/\sqrt{2}$  is where  $|s_m|$  is largest and the required base precision  $\log_{10} |s_m|$  culminates, reaching  $\log_{10} |A_{nm_*} \log 2\xi(2m_*)| \sim \log_{10}(3 + 2\sqrt{2}) n \approx 0.76555 n$  digits, see fig. 11 (vs  $(0.2 \text{ to } 0.3) n$  digits for  $\lambda_n$  [22, fig. 6][17, § 4.2]). Even then, a crude feed of (36) (or (39), (40)) into a mainstream arbitrary-precision system (Mathematica 10 [35]) suffices to reap the  $\Lambda_n$ -values of § 4.1 effortlessly under  $n \approx 20000$ . Our computing times varied erratically but could go down to ca. 4 min for  $\Lambda_{10000}$ , 43 min for  $\Lambda_{20000}$  using (40) (CPU times on an Intel Xeon

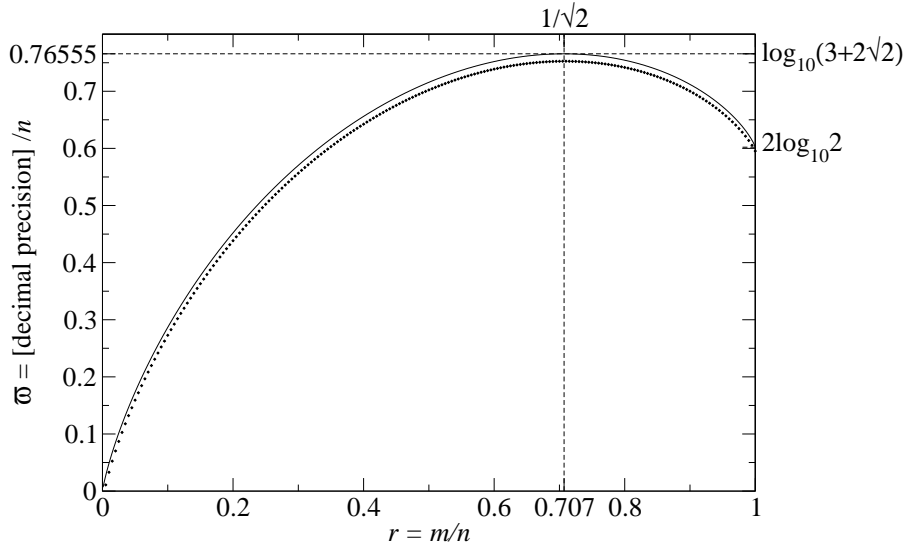


Figure 11: Base decimal precisions needed for the summands of  $\Lambda_n$  in (36), as estimated by  $\log_{10} |A_{nm} \log 2\xi(2m)|$  which is plotted against  $m$  in axes rescaled by  $1/n$ . Dotted curve: the case  $n = 200$ ; continuous curve: the  $n \rightarrow \infty$  limiting form  $\varpi = -2r \log_{10} r + (1+r) \log_{10}(1+r) - (1-r) \log_{10}(1-r)$  ( $r = m/n$ ). (This same form occurs in a seemingly unrelated number-theoretical calculation. [4, § 6.3])

E5-2670 0 @ 2.6 GHz processor).

For higher  $n$ -values, G. Misguich kindly developed a much faster parallel code (available on request), based on the multiple-precision GNU MPFR library, [24] and ran it on a 20-core machine still @ 2.6 GHz with 256 Go of memory. He reached CPU times  $\approx 97$  s for  $n = 20000$ , 5.6 h for  $n = 100000$ , 22.7 days for  $n = 500000$  (without optimizing the precision by fig. 11; thus  $n$  could still be raised, but not so far as to justify the much longer programming and computing times then needed).

Now the true current challenge is to probe  $|T| \gtrsim 2.4 \cdot 10^{12}$  by (4), hence to reach  $n \gtrsim 2 \cdot 10^{36}$  (assuming the more favorable estimate (73),  $10^{60}$  otherwise), which then needs a working precision  $\gtrsim 1.6 \cdot 10^{36}$  decimal places at times. This need for a huge precision already burdened the original  $\lambda_n$  but somewhat less and amidst several steeper complexities; now for the  $\Lambda_n$ , the ill-conditioning increased while other difficulties waned. As current status, the  $n$ -range needed for new tests of RH stays beyond reach for the  $\Lambda_n$  too.

Still,  $\{\Lambda_n\}$  has assets to win over  $\{\lambda_n\}$  in the long run. The  $\Lambda_n$  are fully explicit; their evaluations are recursion-free, thus *very few* samples (at high enough  $n$ , for sure) might suffice to signal that RH is violated *somewhere*; and the required working precision peaking at  $\approx 0.766 n$  stands as the *only* stumbling block, but this is a *purely logistic* barrier, which might be lowered if (36) ever grew better conditioned variants. Already, (39) needs a much lower precision ( $\propto \frac{1}{2} \log_{10} n$ ) for  $\log 2\pi$  as its coefficient  $(2A_{n_0})^{-1} \sim -\frac{1}{2}\sqrt{\pi n}$  grows negligibly, compared to the  $A_{nm} \log(|B_{2m}|/(2m-3)!!)$ : thus only the latter *simpler* expressions demand the top precision, and mainly for  $m \approx n/\sqrt{2}$ . Further such improvements should be pursued in priority to allow for much higher  $n$ . The slow growth of the uncertainty-principle threshold (74) is also an aspect favoring  $\{\Lambda_n\}$ .

## Concluding remark and acknowledgments

While other sequences sensitive to RH for large  $n$  are known [2][14], not to mention Keiper–Li again, we are unaware of any previous case combining a fully *closed form* like (36) with a practical sensitivity-threshold of *tempered growth*  $n = O(T^\nu)$ .

We are very grateful to G. Misguich (from our Institute) who wrote and ran a special fast code for numerical calculations reaching  $n = 500000$ . [24]

## Appendix: Centered variant

We sketch a treatment parallel to the main text for our Li-type sequences using the alternative basepoint  $x_0 = \frac{1}{2}$ , the *center* for the  $\xi$ -function [33, §3.4] (and focusing on the Riemann zeros' case, just for the sake of definiteness).

We recall that the Functional Equation  $\xi(1-x) \equiv \xi(x)$  allows us, in place of the mapping  $z \mapsto x = (1-z)^{-1}$  within  $\xi$  as in (6), to use the double-valued map  $y \mapsto x_{\tilde{w}}(y) = \frac{1}{2} \pm \sqrt{\tilde{w}} y^{1/2}/(1-y)$  (parametrized by  $\tilde{w} > 0$ ) on the unit disk. That still maps the unit circle  $\{|y| = 1\}$  to the completed critical line  $L \cup \{\infty\}$ , but now minus its interval  $\{|\operatorname{Im} x| < \frac{1}{2}\sqrt{\tilde{w}}\}$ . As before, we ask all Riemann zeros on  $L$  to pull back to  $\{|y| = 1\}$ , which imposes  $\tilde{w} < \tilde{w}_0 \stackrel{\text{def}}{=} 4 \min_\rho |\operatorname{Im} \rho|^2 \approx 799.1618$ . We thus define the parametric

sequence  $\{\lambda_n^0(\tilde{w})\}$ , for  $0 < \tilde{w} < \tilde{w}_0$ , by

$$\log 2\xi\left(\frac{1}{2} \pm \frac{\sqrt{\tilde{w}} y^{1/2}}{1-y}\right) \equiv \log 2\xi\left(\frac{1}{2}\right) + \sum_{n=1}^{\infty} \frac{\lambda_n^0(\tilde{w})}{n} y^n \quad (83)$$

([33, §3.4] where only the case  $\tilde{w} = 1$  was detailed, [28]); equivalently,

$$\frac{\lambda_n^0(\tilde{w})}{n} \equiv \frac{1}{2\pi i} \oint \frac{dy}{y^{n+1}} \log 2\xi(x_{\tilde{w}}(y)), \quad n = 1, 2, \dots \quad (84)$$

We now build an *explicit* variant for this sequence (84), similar to  $\{\Lambda_n\}$  for  $\{\lambda_n^K\}$ . First, the deformations of (84) analogous to those in § 2.1 read as

$$\frac{1}{2\pi i} \oint \frac{dy}{H_{y_0}(y) \cdots H_{y_n}(y)} \log 2\xi(x) \quad (\text{here } x \equiv x_{\tilde{w}}(y)), \quad (85)$$

cf. (25), for which the simplest analytical form we found, mirroring (27), is

$$\frac{1}{2\pi i} \oint \frac{2 dr}{(r+1)^2} \prod_{m=0}^n \frac{r+r_m}{r-r_m} \log 2\xi(x), \quad r_m \stackrel{\text{def}}{=} \frac{1+y_m}{1-y_m}, \quad (86)$$

where now  $x \equiv x(r)$  with the new variable

$$r \stackrel{\text{def}}{=} \frac{1+y}{1-y} \equiv [1 + (2x-1)^2/\tilde{w}]^{1/2} \quad (\text{Re } r > 0). \quad (87)$$

Then with  $x_m \equiv 2m$  as before (but now including  $m = 0$ ), the integral (86) evaluated by the residue theorem yields the result (akin to (36))

$$\Lambda_n^0(\tilde{w}) \stackrel{\text{def}}{=} \sum_{m=1}^n \frac{2}{(r_m+1)^2} \frac{\prod_{k=0}^n (r_m+r_k)}{\prod_{k \neq m} (r_m-r_k)} \log 2\xi(2m), \quad r_m \equiv \sqrt{1 + (4m-1)^2/\tilde{w}}. \quad (88)$$

These coefficients, while still explicit, are less tractable than the  $\Lambda_n$  from (36), (32); at the same time their design is more advanced, as it captures the Functional Equation (through the  $\lambda_n^0$ , and unlike the  $\Lambda_n$  and  $\lambda_n$ ); nevertheless we are yet to see any *concrete* benefit to using  $\{\Lambda_n^0\}$  over  $\{\Lambda_n\}$ .

Numerical samples (for  $\tilde{w} = 1$ , closest case to  $\{\Lambda_n\}$ ; compare with (69)):

$$\Lambda_1^0(1) \approx 0.0881535583, \quad \Lambda_2^0(1) \approx 0.237357366, \quad \dots, \quad \Lambda_{2000}^0(1) \approx 6.815307167.$$

The corresponding *asymptotic alternative* for RH analogous to (45)–(47) reads as

- RH false:  $\Lambda_n^0(\tilde{w}) \sim \left\{ \sum_{\operatorname{Re} \rho' > 1/2} \Delta_{\rho'} \Lambda_n^0(\tilde{w}) \right\} \pmod{o(n^\varepsilon) \forall \varepsilon > 0}$  (89)

$$\text{with } \log |\Delta_{\rho'} \Lambda_n^0(\tilde{w})| \sim (\rho' - 1/2) \log n, \quad (90)$$

- RH true:  $\Lambda_n^0(\tilde{w}) \sim \sqrt{\tilde{w}} (\log n + C)$ ,  $C = \frac{1}{2}(\gamma - \log \pi - 1)$  as in (47). (91)

The latter is proved by extending Oesterlé’s method just as with  $\Lambda_n$ ; whereas the former needs large- $n$  estimations of the product in (86), but our current ones remain crude compared to the full Stirling formula available for (30); that precludes us from reaching the absolute scales of the  $\Delta_{\rho'} \Lambda_n^0(\tilde{w})$  and hence the values of  $n$  from which any such terms might become detectable.

Numerically though (with all our tests of § 4 admitting centered variants), we saw all changes from the non-centered data (main text) to be slight, especially for  $n \gg 1$ , aside from the overall factor  $\sqrt{\tilde{w}}$  in (91).

## References

- [1] J. Arias de Reyna, *Asymptotics of Keiper–Li coefficients*, *Funct. Approx. Comment. Math.* **45** (2011) 7–21.
- [2] L. Báez-Duarte, *A sequential Riesz-like criterion for the Riemann Hypothesis*, *Int. J. Math. Math. Sci.* **21** (2005) 3527–3537.
- [3] E.P. Balanzario and J. Sánchez-Ortiz, *Zeros of the Davenport–Heilbronn counterexample*, *Math. Comput.* **76** (2007) 2045–2049.
- [4] G. Beliakov and Y. Matiyasevich, *Approximation of Riemann’s zeta function by finite Dirichlet series: a multiprecision numerical approach*, *Exp. Math.* **24** (2015) 150–161.
- [5] P. Biane, J. Pitman and M. Yor, *Probability laws related to the Jacobi theta and Riemann zeta functions*, *Bull. Amer. Math. Soc.* **38** (2001) 435–465.
- [6] E. Bombieri and A. Ghosh, *Around the Davenport–Heilbronn function*, *Uspekhi Mat. Nauk* **66** (2011) 15–66, *Russian Math. Surveys* **66** (2011) 221–270.

- [7] E. Bombieri and J.C. Lagarias, *Complements to Li's criterion for the Riemann Hypothesis*, J. Number Theory **77** (1999) 274–287.
- [8] M.W. Coffey, *Toward verification of the Riemann Hypothesis: application of the Li criterion*, Math. Phys. Anal. Geom. **8** (2005) 211–255.
- [9] M.W. Coffey, *New results concerning power series expansions of the Riemann xi function and the Li/Keiper constants*, Proc. R. Soc. Lond. **A 464** (2008) 711–731, and refs. therein.
- [10] H. Davenport, *Multiplicative Number Theory*, 3rd ed. revised by H.L. Montgomery, Graduate Texts in Mathematics **74**, Springer (2000), and refs. therein.
- [11] H. Davenport and H. Heilbronn, *On the zeros of certain Dirichlet series I, II*, J. London Math. Soc. **11** (1936) 181–185, 307–312.
- [12] R.B. Dingle, *Asymptotic Expansions: their Derivation and Interpretation*, Academic Press (1973).
- [13] A. Erdélyi, *Asymptotic Expansions*, Dover (1956).
- [14] Ph. Flajolet and L. Vepstas, *On differences of zeta values*, J. Comput. Appl. Math. **220** (2008) 58–73, and refs. therein.
- [15] X. Gourdon, *The  $10^{13}$  first zeros of the Riemann Zeta function, and zeros computation at very large height*, preprint (Oct. 2004), <http://numbers.computation.free.fr/Constants/Miscellaneous/zetazeros1e13-1e24.pdf>
- [16] I.S. Gradshteyn and I.M. Ryzhik, *Table of Integrals, series and products*, 5th ed., A. Jeffrey ed., Academic Press (1994).
- [17] F. Johansson, *Rigorous high-precision computation of the Hurwitz zeta function and its derivatives*, Numer. Algor. **69** (2015) 253–270.
- [18] J.B. Keiper, *Power series expansions of Riemann's  $\xi$  function*, Math. Comput. **58** (1992) 765–773.
- [19] J.C. Lagarias, *Li coefficients for automorphic L-functions*, Ann. Inst. Fourier, Grenoble **57** (2007) 1689–1740.

- [20] X.-J. Li, *The positivity of a sequence of numbers and the Riemann Hypothesis*, J. Number Theory **65** (1997) 325–333.
- [21] K. Maślanka, *Li’s criterion for the Riemann hypothesis — numerical approach*, Opuscula Math. **24** (2004) 103–114.
- [22] K. Maślanka, *Effective method of computing Li’s coefficients and their properties*, preprint (2004), [arXiv:math.NT/0402168](https://arxiv.org/abs/math.NT/0402168) v5.
- [23] K. Maślanka, *Báez-Duarte’s criterion for the Riemann Hypothesis and Rice’s integrals*, preprint (2006), [arXiv:math/0603713](https://arxiv.org/abs/math/0603713) v2 [math.NT].
- [24] G. Misguich, calculations for  $n > 20000$ , using <http://www.mpfr.org/> (private communications, 2017).
- [25] J. Oesterlé, *Régions sans zéros de la fonction zêta de Riemann*, typescript (2000, revised 2001, uncirculated).
- [26] B. Riemann, *Über die Anzahl der Primzahlen unter einer gegebenen Grösse*, Monatsb. Preuss. Akad. Wiss. (Nov. 1859) 671–680 [English translation, by R. Baker, Ch. Christenson and H. Orde: *Bernhard Riemann: Collected Papers*, paper VII, Kendrick Press (2004) 135–143].
- [27] S.K. Sekatskii, *Generalized Bombieri–Lagarias’ theorem and generalized Li’s criterion with its arithmetic interpretation*, Ukr. Mat. Zh. **66** (2014) 371–383, Ukr. Math. J. **66** (2014) 415–431; and: *Asymptotic of the generalized Li’s sums which non-negativity is equivalent to the Riemann Hypothesis*, [arXiv:1403.4484](https://arxiv.org/abs/1403.4484) [math.NT] (2014).
- [28] S.K. Sekatskii, *Analysis of Voros criterion equivalent to Riemann Hypothesis*, Analysis, Geometry and Number Theory **1** (2016) 95–102; [arXiv:1407.5758](https://arxiv.org/abs/1407.5758) [math.NT].
- [29] R. Spira, *Some zeros of the Titchmarsh counterexample*, Math. Comput. **63** (1994) 747–748.
- [30] E.C. Titchmarsh, *The Theory of the Riemann Zeta-Function* (2nd ed., revised by D.R. Heath-Brown), Oxford Univ. Press (1986).
- [31] A. Voros, *A sharpening of Li’s criterion for the Riemann Hypothesis*, preprint (Saclay-T04/040 April 2004, unpublished, [arXiv:](https://arxiv.org/abs/)

- math.NT/0404213 v2), and *Sharpenings of Li's criterion for the Riemann Hypothesis*, Math. Phys. Anal. Geom. **9** (2006) 53–63. <sup>3</sup>
- [32] A. Voros, *Zeta functions over zeros of zeta functions*, Lecture Notes of the Unione Matematica Italiana **8**, Springer-Verlag (2010) chap. 11. <sup>3</sup>
- [33] A. Voros, *Zeta functions over zeros of Zeta functions and an exponential-asymptotic view of the Riemann Hypothesis*, in: *Exponential Analysis of Differential Equations and Related Topics* (Proceedings, Kyoto, oct. 2013, ed. Y. Takei), RIMS Kôkyûroku Bessatsu **B52** (2014) 147–164, arXiv:1403.4558 [math.NT].
- [34] A. Voros, *An asymptotic criterion in an explicit sequence*, preprint IPhT15/106 (June 2015), HAL archive: cea-01166324, and *Simplifications of the Keiper/Li approach to the Riemann Hypothesis*, IPhT16/011 (Feb. 2016), arXiv:1602.03292 [math.NT]<sup>4</sup> (unpublished).
- [35] S. Wolfram, Mathematica, 3rd ed., Wolfram Media/Cambridge University Press (1996).

---

<sup>3</sup>Erratum: our asymptotic statements for  $\lambda_n$  in the RH false case have wrong sign.

<sup>4</sup>Eqs. (35), (40), (51) have typos, fixed in the present work.